

# Geometric and solvent effects on intramolecular phenolic hydrogen abstraction by carbonyl $n,\pi^*$ and $\pi,\pi^*$ triplets

Edward C. Lathioor and William J. Leigh

**Abstract:** The photochemistry of a series of alkoxyacetophenone, -benzophenone, and -indanone derivatives, which contain a remote phenolic group linked to the ketone by a *para,para'*- or *meta,meta'*-oxyethyl spacer, has been studied in acetonitrile and dichloromethane solutions using laser flash photolysis techniques. The corresponding methoxy-substituted compounds and, in the case of the alkoxyindanones, derivatives bearing just a remote phenyl substituent, have also been examined. The triplet lifetimes of the phenolic compounds are determined by the rates of intramolecular abstraction of the remote phenolic hydrogen, and depend on the solvent, the geometry of attachment and the configuration of the lowest triplet state. In contrast to the large (>500-fold) difference in lifetime of the *para,para'*- and *meta,meta'*-alkoxyacetophenone derivatives, both of which have lowest  $\pi,\pi^*$  triplet states, smaller differences are observed for the alkoxyindanone (lowest charge transfer triplet, ~twofold difference) and alkoxybenzophenone (lowest  $n,\pi^*$  triplet, ~18-fold difference) derivatives in acetonitrile solution. The triplet lifetimes of the acetophenone and benzophenone are significantly shorter in dichloromethane than in acetonitrile, consistent with the intermediacy of a hydrogen-bonded triplet exciplex in the reaction. This is not the case with the *para,para'*-indanone derivative, suggesting that hydrogen abstraction in this compound is dominated by a mechanism involving initial charge transfer rather than hydrogen bonding. This is most likely due to orientational constraints that prevent the remote phenolic -O-H group from adopting a coplanar arrangement with the  $n$ -orbitals of the carbonyl group.

**Key words:** photochemistry, aromatic ketone, phenol, triplet, intramolecular, quenching, hydrogen abstraction, phenoxy radical, kinetics, kinetic isotope effect, laser flash photolysis.

**Résumé :** Faisant appel à des techniques de photolyse éclair au laser et opérant dans des solutions d'acétonitrile et de dichlorométhane, on a étudié la photochimie d'une série de dérivés alkoxyacétophénones, -benzophénones et -indanones comportant un groupe phénolique dans une position éloignée, mais liée à la cétone par un espaceur oxyéthyle en *para,para'*- ou *méta,méta'*-. On a aussi étudié les composés correspondants portant des substituants méthoxy ainsi que, dans le cas des alkoxyindanones, des dérivés ne portant qu'un substituant phényle en position éloignée. On a déterminé les temps de vie du triplet des composés phénoliques à partir des vitesses d'enlèvement intramoléculaire de l'hydrogène phénolique éloigné; ils dépendent du solvant, de la géométrie de fixation et de la configuration de l'état triplet le plus bas. Par opposition à la grande différence (>500 fois) dans les temps de vie des dérivés *para,para'*- et *méta,méta'*-alkoxyacétophénones qui ont tous les deux des états triplets  $\pi,\pi^*$  plus faibles, on observe des différences plus faibles pour les dérivés alkoxyindanones (triplet de transfert de charge le plus faible; différence du simple au double) et alkoxybenzophénones (triplet  $n,\pi^*$  le plus faible; différence correspondant à une réaction environ 18 fois plus rapide) dans une solution d'acétonitrile. Les temps de vie des dérivés de l'acétophénone et de la benzophénone sont beaucoup plus courts en solution dans le dichlorométhane que dans l'acétonitrile; ce résultat est en accord avec une réaction se produisant par l'intermédiaire d'un exciplex triplet avec liaison hydrogène. Ce n'est pas le cas pour le dérivé *para,para'*-indanone et ce résultat suggère l'enlèvement de l'hydrogène dans ce composé est dominé par un mécanisme impliquant dans un premier temps un transfert de charge plutôt que la formation d'une liaison hydrogène. Cette différence résulte vraisemblablement de contraintes qui font que le groupe -O-H phénolique éloigné ne peut s'orienter dans un arrangement coplanaire avec les orbitales  $n$  du groupe carbonyle.

**Mots clés :** photochimie, cétone aromatique, phénol, triplet, intramoléculaire, piégeage, enlèvement d'hydrogène, radical phénoxy, cinétique, effet isotopique cinétique, photolyse éclair au laser.

[Traduit par la Rédaction]

Received June 18, 2001. Published on the NRC Research Press Web site at <http://canjchem.nrc.ca> on December 10, 2001.

**E.C. Lathioor and W.J. Leigh.**<sup>1</sup> Department of Chemistry, McMaster University, 1280 Main Street West, Hamilton, ON L8S 4M1, Canada.

<sup>1</sup>Corresponding author (fax: (905) 522-2509; e-mail: [leigh@mcmaster.ca](mailto:leigh@mcmaster.ca)).

## Introduction

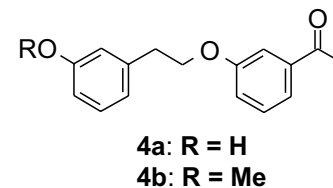
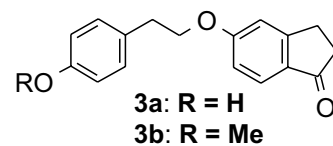
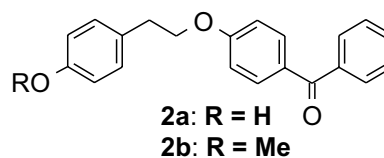
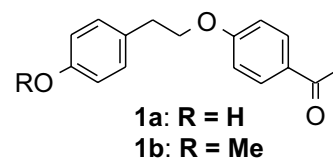
Hydrogen abstraction from phenols by the excited triplet states of most aromatic ketones occurs at rates in excess of  $1 \times 10^9 \text{ M}^{-1} \text{ s}^{-1}$  in solution, resulting in the formation of the corresponding phenoxy and hemipinacol radicals in close to unit quantum yields (1–6). Unlike hydrogen abstraction from alkanes, alcohols, or substituted toluenes (7), however, the

normal dependence of the rate constant for reaction on the configuration of the lowest triplet state is not observed, and ketones with lowest  $\pi,\pi^*$  triplet states tend to exhibit greater reactivity than those with lowest  $n,\pi^*$  triplets. This characteristic is suggestive of an electron-transfer mechanism, where the hydrogen atom is transferred as a proton after initial electron transfer to yield the corresponding  $\text{PhOH}^+/\text{Ar}_2\text{CO}^-$  radical ion pair. While recent work suggests that this is indeed the mechanism followed by benzophenone and other aromatic ketones in pure water (8, 9), electron transfer is more endergonic in nonaqueous solvents, where the reduction potentials of ketones are higher than in hydroxylic media (10). To be sure, previous kinetic studies indicate that the situation in nonaqueous solvents is generally more complicated than a simple electron transfer mechanism can accommodate (3, 11).

We have recently proposed that in acetonitrile solution, quenching of  $\pi,\pi^*$  aromatic ketone triplets proceeds via electron and (or) proton transfer within a hydrogen-bonded triplet exciplex, in which the hydrogen bond serves mainly to facilitate electron transfer from the phenol to the ketone by lowering the oxidation and reduction potentials of the redox pair (11). Phenolic quenching of ketones with lowest  $n,\pi^*$  triplet states was suggested to proceed by two mechanisms, depending on the triplet state reduction potential and the proximity of the higher lying  $\pi,\pi^*$  triplet state, on the basis of the observation of a V-shaped Hammett plot for the quenching of a series of substituted benzophenone triplets by *para*-cresol. Electron-acceptor-substituted benzophenone derivatives were proposed to be quenched by the charge-transfer exciplex mechanism common to abstraction from substituted toluenes (12–15), which presumably transforms into the “simple” electron transfer mechanism when the reduction potential of the ketone is low enough. Quenching of electron-donor-substituted derivatives, on the other hand, was proposed to proceed via the hydrogen-bonded exciplex mechanism and involve the higher lying, relatively basic  $\pi,\pi^*$  triplet state.

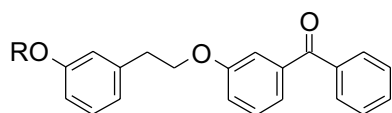
Phenolic quenching of aromatic ketone triplets also occurs intramolecularly, as has been demonstrated in a study of the photochemistry of the oxyethyl-linked phenolic ketones **1a–3a** (11, 16, 17). The triplet lifetimes of these compounds in acetonitrile solution at room temperature are in the 10–30 ns range, orders of magnitude shorter than the corresponding methoxy-substituted analogues (**1b–3b**), and they vary throughout the series in a similar way as do the rate constants for bimolecular quenching of the corresponding (methoxy-substituted) model compounds by *para*-cresol under the same conditions (11). Surprisingly, this correlation fails for the *meta,meta'*-analogue of the phenolic acetophenone derivative **1a**, 3-[2-(3'-hydroxyphenyl)ethoxy]acetophenone (**4a**) (18). The triplet lifetime of this compound exceeds 10  $\mu\text{s}$  in acetonitrile solution at 23°C and is similar to that of the methoxy analogue **4b**, indicating that intramolecular abstraction of the remote phenolic hydrogen is over 500 times slower in this compound than in **1a**. The rate constant for the analogous bimolecular reaction is quite fast, so the very low reactivity of the triplet state of **4a** must be due to specific geometrical factors that are not present in the *para,para'*-derivative **1a**. Molecular mechanics calculations indicate that **4a** can adopt several conformations in which

the phenolic hydrogen is within abstracting distance (less than ca. 2.65 Å) of the carbonyl oxygen, but in which there is little or no overlap between the aryl rings. We have proposed that the much longer lifetime of **4a** is due to the preferred formation of one or more of these exciplex conformers, in which quenching is presumably relatively slow, as well as orbital symmetry restrictions to electron and (or) proton transfer in the (higher energy) sandwich-like conformer similar to the one that must be involved in intramolecular hydrogen abstraction in **1a**.

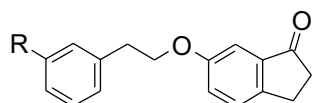


In the present paper, we report the results of further studies of the role of geometrical factors in intramolecular phenolic hydrogen abstraction by aromatic ketone triplets, and the effects of solvent polarity on the rate constants. We have thus prepared two new phenolic ketones (**5a** and **6a**), which feature the same *meta,meta'*-linkage as is present in **4a**, and have examined their photochemistry under similar conditions as the *para,para'*-analogues **2a** and **3a**. As with **1a–3a**, the main difference between the three *meta,meta'*-substituted compounds (**4a–6a**) is the configuration of the lowest triplet state ( $\pi,\pi^*$  in **4a** and **6a**;  $n,\pi^*$  in **5a**). Further, **4a** and **6a** differ in the degree of charge-transfer character associated with their lowest  $\pi,\pi^*$  triplet states, an effect which is due to the differing abilities of the carbonyl group to twist out of the plane of its attached aromatic ring in the two molecules. As before, the role of intramolecular hydrogen abstraction in controlling the triplet lifetimes of the two compounds is assessed through a comparison to the triplet state behavior of the corresponding methoxy-analogues (**5b** and **6b**, respectively), and in the case of the indanone derivatives, to the phenyl-substituted analogues **6c** and **7** as well. Finally, the triplet state behavior of the entire series of compounds (**1–7**), as well as rate constants for bimolecular phenolic hydro-

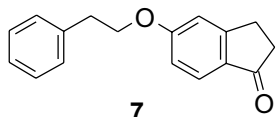
gen abstraction in appropriate model compounds, have been determined in dichloromethane solution. Comparison of these data to those in acetonitrile solution allows an assessment of the effects of (aprotic) solvent polarity on the rates of both inter- and intramolecular versions of the reaction.



**5a:** R = H  
**5b:** R = Me



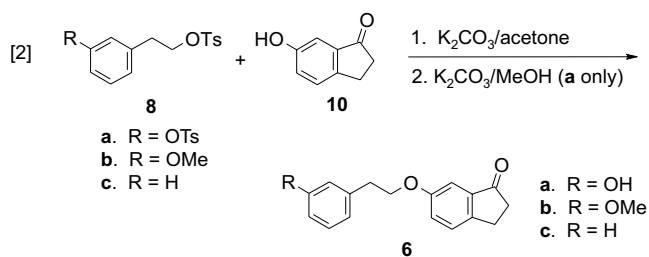
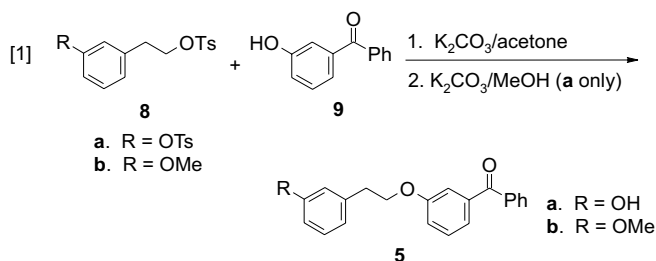
**6a:** R = OH  
**6b:** R = OMe  
**6c:** R = H



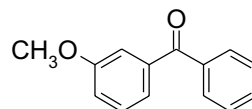
**7**

## Results

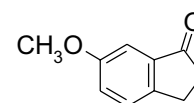
Compounds **5a** and **6a** were prepared by reaction of the ditosylate ester of 3-hydroxy- $\beta$ -phenethyl alcohol (**8a**) with 3-hydroxybenzophenone (**9**) and 6-hydroxy-1-indanone (**10**), respectively, in acetone solution, followed by alkaline hydrolysis in methanol (eqs. [1] and [2]). The others (**5b**, **6b**, **6c**, and **7**) were prepared in similar fashion, by reaction of the tosylate esters of 3-methoxy- $\beta$ -phenethyl alcohol (**8b**) or  $\beta$ -phenethyl alcohol (**8c**) with **9**, **10**, or 5-hydroxy-1-indanone (**11**). The structures of **5–7** were assigned on the basis of their  $^1\text{H}$  and  $^{13}\text{C}$  NMR, IR and mass spectra, and combustion analyses.



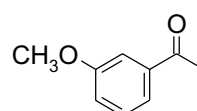
As was found previously for **1–4** (11, 18), ultraviolet absorption spectra of **5** and **6** in acetonitrile were in each case indistinguishable from those of the corresponding model compounds **12** and **13**, indicating that no ground-state interactions exist between the carbonyl group and the remote aryl group in these molecules. The same conclusion was derived from comparison of the UV absorption spectra of **1–7** with those of the corresponding model compounds (**12–17**) in dichloromethane solution.



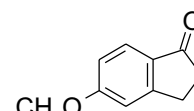
**12**



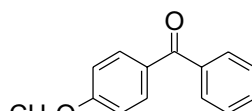
**13**



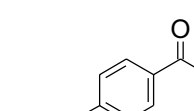
**14**



**15**



**16**



**17**

Phosphorescence emission spectra of **5a** and **6a** were recorded in 4:1 ethanol:methanol glasses at 77 K, with similar measurements made on the model compounds for comparison. The spectra of **5a**, **5b**, and **12** were similar, as were those of **6a**, **6b**, and **13**. Triplet energies were estimated from the short wavelength onset of the 0–0 emission bands in the spectra; these are  $68.3 \pm 0.3 \text{ kcal mol}^{-1}$  for **5a**, **b** and  $71.4 \pm 0.1 \text{ kcal mol}^{-1}$  for **6a**, **b**. The appearance of the spectra are consistent with an  $n,\pi^*$  assignment for the lowest triplet states of **5a**, **b**, and a  $\pi,\pi^*$  assignment for **6a**, **b**.

Steady state photolyses (300 nm) were carried out on deoxygenated 0.0025 M acetonitrile solutions of **5a** and **6a**, with periodic monitoring of the solutions by gas chromatography. As observed previously for **1a–3a** (11, 18), no photoproducts of similar or lower molecular weight to the starting ketones could be detected in any case. Exhaustive irradiation of the solutions produced small amounts of high molecular weight materials. Quantum yields for substrate photolysis were estimated to be in the 0.001–0.01 range using the disappearance of **1a** ( $\Phi = 0.006$ ) (16) as actinometer. Compounds **5b** and **6b** were found to be similarly unreactive.

Nanosecond laser flash photolysis (NLFP) experiments employed a pulsed excimer laser filled with  $\text{N}_2\text{-He}$  (337 nm, 4 mJ, 6 ns),  $\text{Xe-HCl-He}$  (308 nm, 55 mJ, 15 ns), or  $\text{Kr-F}_2\text{-N}$  (248 nm, 100 mJ, 25 ns) for excitation, and a microcomputer-controlled detection system (19). Sample concentrations were such that the absorbance at the excitation wavelength (3- or 7-mm path length) was 0.2–0.9 and each sample was deoxygenated with argon or dry nitrogen until constant transient lifetimes were obtained.

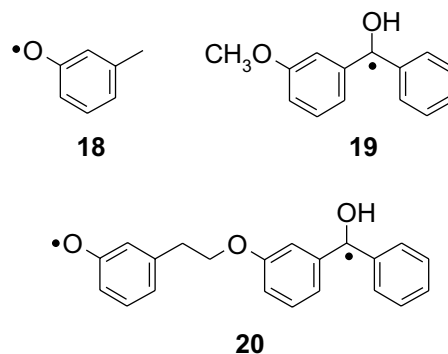
Absolute rate constants for bimolecular quenching of the triplet states of **12–17** by *para*- or *meta*-cresol were determined in acetonitrile and (or) dichloromethane solution at 23–25°C using the 337 nm laser for excitation. In each case, the pseudo-first-order triplet decay rate constant ( $k_{\text{decay}}$ ) was determined at or near the triplet–triplet absorption maximum (380 nm for the acetophenone and indanone derivatives; 525 or 600 nm for the benzophenone derivatives) as a function of concentration of added phenol. Addition of the phenols resulted in an increase in triplet decay rate and the formation of new, long-lived absorptions assignable to *para*- or *meta*-cresyloxy radicals and the corresponding hemipinacol radicals. While these absorptions overlap with those due to the ketone triplets at 380 nm, they were sufficiently long-lived that triplet decay rate constants could generally be determined with reasonable accuracy by simply taking the absorption due to the radical products as the infinity level in the least-squares analyses of the  $\Delta\text{OD}$  vs. time data. At low phenol concentrations where the triplet lifetime was only  $\leq 5$  times shorter than those of the radicals, the triplet decay rates were determined by two-exponential least-squares fitting of the data. Bimolecular quenching rate constants ( $k_q$ ) were determined from plots of the ketone triplet decay rate ( $k_{\text{decay}}$ ) vs. cresol concentration ( $[\text{Q}]$ ) according to eq. [3], where  $k_0$  is the pseudo-first-order rate constant for triplet decay in the absence of quencher. The results of these experiments are collected in Table 1.

$$[3] \quad k_{\text{decay}} = k_0 + k_q[\text{Q}]$$

Laser flash photolysis of solutions of the non-phenolic ketones **5b**, **6b**, **c**, and **7** in deoxygenated, dry acetonitrile solution led to the formation of strongly absorbing transients which decayed with clean pseudo-first-order kinetics (at low laser intensities) and exhibited lifetimes in the 1–10  $\mu\text{s}$  range. These were assigned to the corresponding triplet states on the basis of their absorption spectra, which were indistinguishable from those of the corresponding model compounds (**12** in the case of **5b**, **13** in the case of **6b** and **6c**, and **15** in the case of **7**), and the fact that they are quenched rapidly by 1,3-cyclohexadiene (CHD,  $k_q = 6\text{--}9 \times 10^9 \text{ M}^{-1} \text{ s}^{-1}$ ) and oxygen ( $k_q > 1 \times 10^9 \text{ M}^{-1} \text{ s}^{-1}$ ). The triplet–triplet absorption spectra of **5b** and **6b** in acetonitrile are shown in Fig. 1, while the inserts show typical decay profiles recorded at 600 and 385 nm, respectively. The spectra shown were recorded over ca. 200 ns time windows, starting just after the peak in the transient decay profiles.

The transient absorption spectra from flash photolysis of the phenolic ketones **5a** and **6a** are significantly different from those of the corresponding methoxy analogues. For example, Fig. 2a shows the spectra obtained from a  $2.2 \times 10^{-4} \text{ M}$  solution of **5a** in acetonitrile ( $\lambda_{\text{exc}} = 248 \text{ nm}$ ), at the point corresponding to the peak in the transient decay profile and over the 0.5–1.0  $\mu\text{s}$  time window after the peak. For comparison, spectra recorded of an acetonitrile solution containing **12** (0.0076 M) and *meta*-cresol (0.0058 M) over similar time windows, using the 337 nm laser for excitation, are shown in Fig. 2b. The early spectrum of Fig. 2b is a superposition of spectra due to the triplet state of **12** ( $\lambda_{\text{max}} = 330 \text{ nm}$ , plus a broad absorption centered at  $\lambda \sim 530 \text{ nm}$ ) and the monoradicals **18** ( $\lambda_{\text{max}} = 405 \text{ nm}$ ) and **19** ( $\lambda_{\text{max}} = 330, 545 \text{ nm}$ ), while that recorded at later times is due to **18** and **19** alone.

The spectra of Fig. 2a can thus be assigned to mixtures of the triplet state of **5a** and biradical **20**, with the later spectrum consisting of a correspondingly greater proportion of biradical relative to triplet. The decays followed clean pseudo-first-order kinetics at all wavelengths between 300 and 700 nm, but exhibited different lifetimes and quenching behavior depending on the monitoring wavelength. Decays recorded above 600 nm exhibited a lifetime of  $\sim 280 \text{ ns}$  and were quenched cleanly by CHD ( $k_q = 7.5 \times 10^9 \text{ M}^{-1} \text{ s}^{-1}$ ), indicating them to be due to the triplet state of the ketone exclusively. Those recorded at 520 or 300 nm exhibited lifetimes of  $\sim 850 \text{ ns}$ ; the lifetime did not change upon addition of the diene, although the intensities of the absorptions appeared to decrease as the diene concentration was increased. This behavior suggests that the transient absorptions in the 300–550 nm region of the spectrum are mainly due to the biradical (**20**), which is formed by intramolecular hydrogen abstraction in the triplet state of the ketone. Oxygen quenched the lifetime of the transient absorptions throughout the complete range of the spectrum, with a rate constant  $k_{\text{O}_2} \sim 1 \times 10^9 \text{ M}^{-1} \text{ s}^{-1}$ .



As expected, the triplet lifetime of **5a** (measured at 600 nm) varies with the concentration of the ketone. Figure 3 shows a plot of the triplet decay rate constant ( $\tau_T^{-1}$ ) vs. [**5a**] in deoxygenated acetonitrile solution at 25.0°C. The intercept of the plot affords the infinite dilution triplet lifetime ( $\tau_T = 362 \pm 16 \text{ ns}$ ) while the slope is the bimolecular rate constant for self-quenching of the triplet state of **5a** by the ground state ketone ( $k_{\text{sq}} = (2.2 \pm 0.4) \times 10^9 \text{ M}^{-1} \text{ s}^{-1}$ ). The latter agrees quite well with the bimolecular rate constant for quenching of the triplet state of 3-methoxybenzophenone (**12**) by *meta*-cresol under similar conditions (Table 1).

The transient absorption spectrum obtained from 248 nm laser flash photolysis of **6a** under similar conditions is shown in Fig. 4. In this case, however, the spectrum changes imperceptibly (other than in intensity) with time, and there is no variation in lifetime ( $\tau \sim 630 \text{ ns}$ ) throughout the wavelength range monitored. The lifetime of the absorption is shortened upon addition of oxygen ( $k_{\text{O}_2} \sim 1 \times 10^9 \text{ M}^{-1} \text{ s}^{-1}$ ), but addition of CHD resulted only in reductions in the initial transient absorbance ( $\Delta\text{OD}_{\text{max}}$ ) at each wavelength, to an extent that depends on the concentration of CHD added. This behavior indicates that the species is a product of the triplet state of the ketone, and we hence assign it to biradical **21**. As expected, the spectrum is similar to that of a mixture of the analogous monoradicals **18** and **22**, generated by 308 nm flash photolysis of **13** (0.001 M) and *meta*-cresol (0.0011 M) in acetonitrile (not shown).

**Table 1.** Absolute rate constants for quenching of ketone triplets by *para*- and *meta*-cresol in acetonitrile (MeCN) and dichloromethane (DCM) at 23–25°C, in units of  $1 \times 10^9 \text{ M}^{-1} \text{ s}^{-1}$ .<sup>a</sup>

Ketone	$k_q$ (MeCN)		$k_q$ (DCM)	
	<i>para</i> -Cresol	<i>meta</i> -Cresol	<i>para</i> -Cresol	<i>meta</i> -Cresol
4-Methoxy acetophenone ( <b>17</b> )	$1.14 \pm 0.09$	$0.71 \pm 0.02^b$	$5.51 \pm 0.10$	—
3-Methoxy acetophenone ( <b>14</b> )	$1.32 \pm 0.04^b$	$1.06 \pm 0.05^b$	—	$5.4 \pm 0.3$
4-Methoxy benzophenone ( <b>16</b> )	$1.17 \pm 0.06^{c,d}$	$0.96 \pm 0.05^e$	$6.5 \pm 0.3$	—
3-Methoxy benzophenone ( <b>12</b> )	$2.01 \pm 0.15$	$1.66 \pm 0.09$	—	$5.4 \pm 0.2$
5-Methoxy-1-indanone ( <b>15</b> )	$1.74 \pm 0.13^c$	$0.88 \pm 0.09$	$7.1 \pm 0.2$	—
6-Methoxy-1-indanone ( <b>13</b> )	$2.18 \pm 0.11$	$1.69 \pm 0.05$	—	$5.3 \pm 0.2$

<sup>a</sup>Measured by 337 nm laser flash photolysis of 0.01–0.03 M solutions of the ketones in deoxygenated acetonitrile. In units of  $1 \times 10^9 \text{ M}^{-1} \text{ s}^{-1}$ .

<sup>b</sup>From ref. 18.

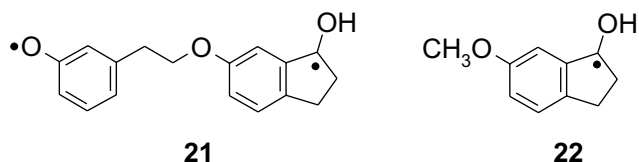
<sup>c</sup>From ref. 11.

<sup>d</sup>Measured at 27°C.

<sup>e</sup>Measured at 29°C.

Figure 5 shows a Stern–Volmer plot of the maximum signal intensities at 385 nm ( $\Delta\text{OD}_{\text{max}}$ ) obtained by flash photolysis of **6a** in the presence of CHD at various concentrations. The data were analyzed according to eq. [4], where  $(\Delta\text{OD}_{\text{max}})_0$  is the value in the absence of diene,  $(\Delta\text{OD}_{\text{max}})_{[Q]}$  is the value in the presence of diene at concentration  $[Q]$ ,  $k_q$  is the rate constant for quenching of the triplet state of the ketone by the diene, and  $\tau_T$  is the ketone triplet lifetime. A triplet lifetime of  $\tau_T = 53 \pm 5 \text{ ns}$  was obtained from the slope of the plot ( $k_q\tau_T = 564 \pm 42 \text{ M}^{-1}$ ), using a value of  $k_q = 1.05 \times 10^{10} \text{ M}^{-1} \text{ s}^{-1}$ , the rate constant for bimolecular quenching of the triplet state of **13** by CHD in acetonitrile at 23°C.

$$[4] \quad (\Delta\text{OD}_{\text{max}})_0 / (\Delta\text{OD}_{\text{max}})_{[Q]} = 1 + k_q\tau_T[Q]$$



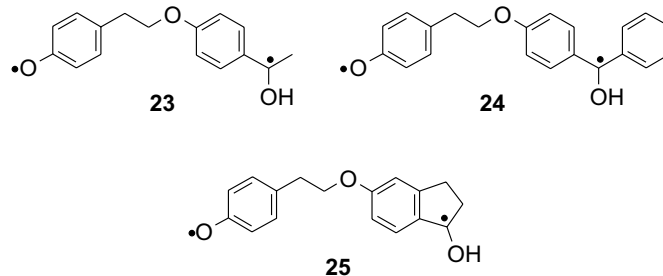
Addition of 0.028 M  $\text{H}_2\text{O}$  or  $\text{D}_2\text{O}$  to the acetonitrile solutions of **5a** and **6a** resulted in small changes in triplet lifetime (determined in the same fashion as described above) compared to those obtained in the dry solvent, but the lifetimes were slightly greater in  $\text{D}_2\text{O}$ –MeCN than in  $\text{H}_2\text{O}$ –MeCN. Table 2 lists the triplet lifetimes determined for **5**–**7** under the three sets of conditions,  $k_H/k_D$  values calculated from the lifetimes in wet acetonitrile, and the analogous data for **1**–**4** (11) for purposes of comparison.

Laser flash photolysis of **1**–**7** in deoxygenated dichloromethane solution afforded similar results to those obtained in acetonitrile (see above and ref. 11), and triplet lifetimes were measured in analogous fashion in each case. Those of the non-phenolic ketones (**1b**–**6b**, **6c**, and **7**) and the phenolic compounds **4a** and **5a** were long enough that they could be measured directly, and so they were determined using the 248 nm laser and solutions containing  $\sim 2 \times 10^{-4} \text{ M}$  ketone. Doubling the concentration of ketone had no discernible effect on the lifetime of **5a** but did in the case of **4a**, so the infinite dilution lifetime was estimated from a plot of  $\tau_T^{-1}$  vs.  $[\mathbf{4a}]$ , constructed from solutions of various concentrations up to  $\sim 0.002 \text{ M}$  and using the 308 or 337 nm lasers for solutions of higher concentrations. The data afforded a value of

$k_{\text{sq}} = (4.6 \pm 0.8) \times 10^9 \text{ M}^{-1} \text{ s}^{-1}$  for the self-quenching rate constant and an infinite dilution triplet lifetime of  $\tau_T = 1.6 \pm 0.3 \mu\text{s}$  at 23°C.

Only biradical absorptions could be detected in the cases of **1a**–**3a** and **6a** in dichloromethane, as shown by the response of the signals to added oxygen and CHD. Thus, triplet lifetimes were determined either by Stern–Volmer quenching with CHD (**3a** and **6a**) or the 1-methylnaphthalene (MN) probe technique (20) (**1a** and **2a**) (21), with solutions containing  $\sim 0.01 \text{ M}$  ketone and using the 337 nm laser for excitation. For example, Fig. 6 shows plots of  $\Delta\text{OD}_{\text{max}}$  at 425 nm (the maximum in the triplet–triplet absorption spectrum of MN) vs.  $[\text{MN}]$  for **1a** and **3a**. The solid lines in the plots represent the best fit of the data to the expression of eq. [5], where  $C$  is a constant proportional to the pathlength, the extinction coefficient of the MN triplet–triplet absorption at 425 nm, the light intensity, and the intersystem crossing yield of the ketone triplet. Triplet lifetimes were calculated from the Stern–Volmer constants ( $k_q\tau_T$ ) using a value of  $k_q = (7.5 \pm 0.4) \times 10^9 \text{ M}^{-1} \text{ s}^{-1}$  for the rate constant for ketone triplet quenching by MN, determined for ketones **16** and **17** under similar conditions. The dichloromethane data for **1**–**7** are listed in Table 2 along with those for acetonitrile solution. Table 3 lists the lifetimes of the phenoxy-hemipinacol biradicals **20**, **21**, and **23**–**25** in the two solvents.

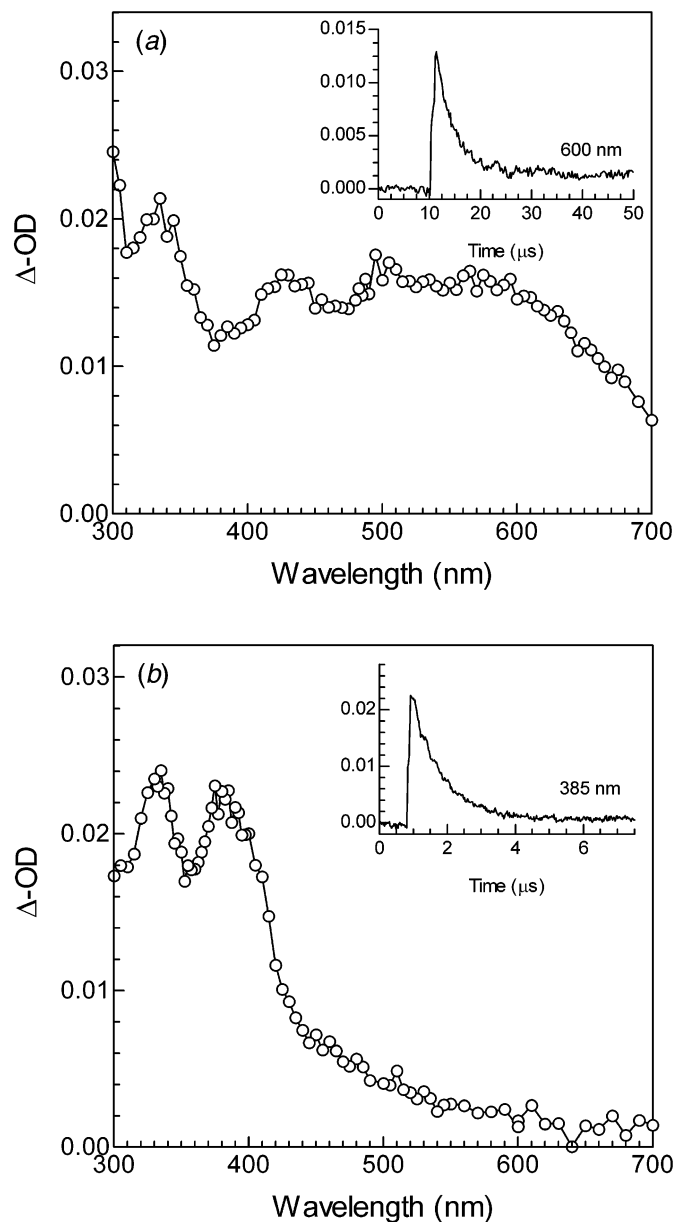
$$[5] \quad \Delta\text{OD}_{\text{max}} = Ck_q\tau_T[\text{MN}] / (1 + k_q\tau_T[\text{MN}])$$



## Discussion

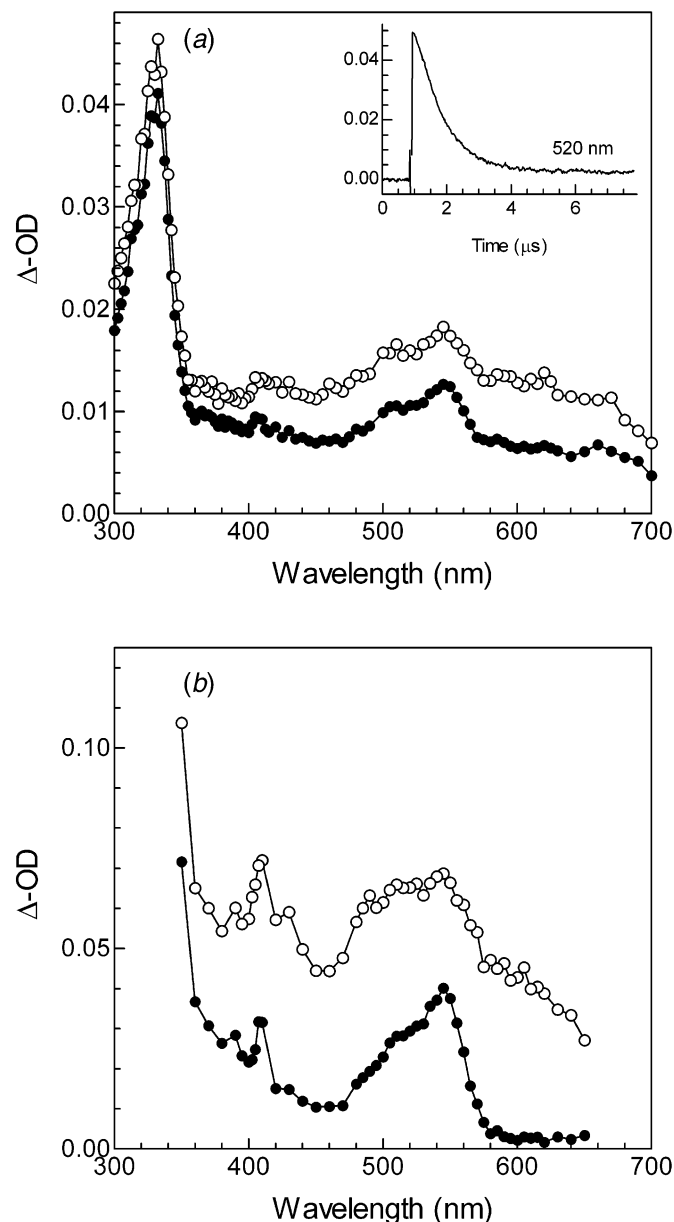
From the transient spectra, isotope effects on the triplet lifetimes, and a comparison of the triplet lifetimes of the phenolic compounds **5a** and **6a** with those of their methoxy analogues **5b** and **6b**, it is clear that triplet state deactivation

**Fig. 1.** Transient absorption spectra from laser flash photolysis of deoxygenated  $\sim 1 \times 10^{-4}$  M acetonitrile solutions of **5b** (a) and **6b** (b) at  $25.0 \pm 0.2^\circ\text{C}$ . The inserts show decay traces monitored at 600 nm (**5b**) and 385 nm (**6b**).



in the two phenolic ketones is dominated by remote phenolic hydrogen atom abstraction, as we found previously for **1a–3a** (11). Both ketones exhibit significantly longer triplet lifetimes than their *para,para*-positional isomers (**2a** and **3a**, respectively) in dry acetonitrile, but in contrast to the situation with the acetophenone derivatives **1a** and **4a** ( $\tau_T^{4a}/\tau_T^{1a} \geq 500$ ) (18), the geometric dependence of the rates is much smaller in the benzophenone ( $\tau_T^{5a}/\tau_T^{2a} \sim 18$ ) and indanone ( $\tau_T^{6a}/\tau_T^{3a} \sim 2.5$ ) derivatives. As the data in Table 1 show, these differences are well beyond what might be expected on the basis of the (small) differences in the rate constants for the corresponding bimolecular hydrogen abstraction processes. The individual triplet lifetimes of the acetophenone and benzophenone derivatives are consistently shorter in dichloro-

**Fig. 2.** (a) Transient absorption spectra from 248 nm laser flash photolysis of a deoxygenated  $2 \times 10^{-4}$  M solution of the phenolic ketone **5a** in dry acetonitrile solution at  $25.0 \pm 0.2^\circ\text{C}$ , at the peak of the decay profile (○) and 0.5 to 1.0  $\mu\text{s}$  later (●). The insert shows a typical decay trace, recorded at a monitoring wavelength of 520 nm. (b) Transient absorption spectra from 337 nm laser flash photolysis of an acetonitrile solution containing *meta*-methoxybenzophenone (**12**, 0.0076 M) and *meta*-cresol (0.0058 M) at  $23.0 \pm 0.2^\circ\text{C}$ , 75–85 ns (○) and 4.0 to 4.3  $\mu\text{s}$  (●) after the pulse.



methane than in acetonitrile solution, but the differences between *para,para*'- and *meta,meta*'-positional isomers follow the same trends in the two solvents; in dichloromethane at  $23^\circ\text{C}$ , the lifetime ratios are a  $\tau_T^{4a}/\tau_T^{1a} \sim 800$ ,  $\tau_T^{5a}/\tau_T^{2a} \sim 25$  for the acetophenone and benzophenone derivatives, respectively. In contrast, the corresponding lifetime ratio for the indanone derivatives is inverted in dichloromethane relative to acetonitrile.

**Fig. 3.** Plot of  $k_{\text{decay}}$  vs. ketone concentration for the triplet state of **5a** in dry acetonitrile at 25°C, monitored at 600 nm.

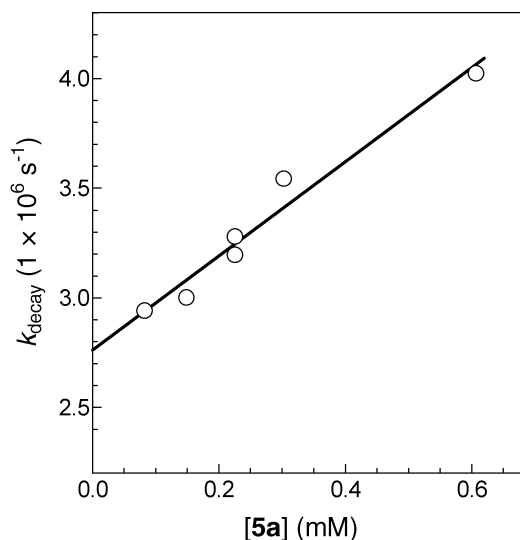
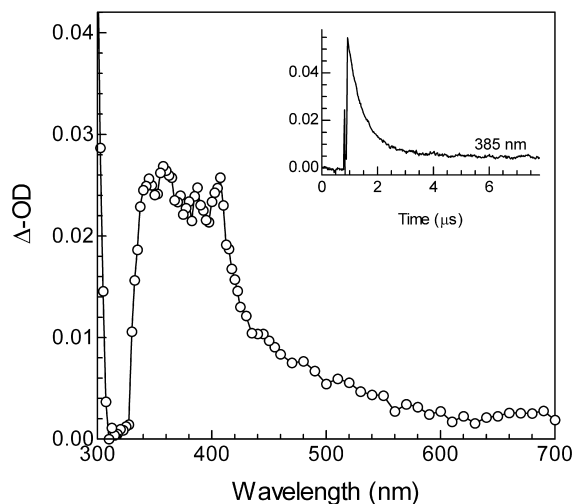
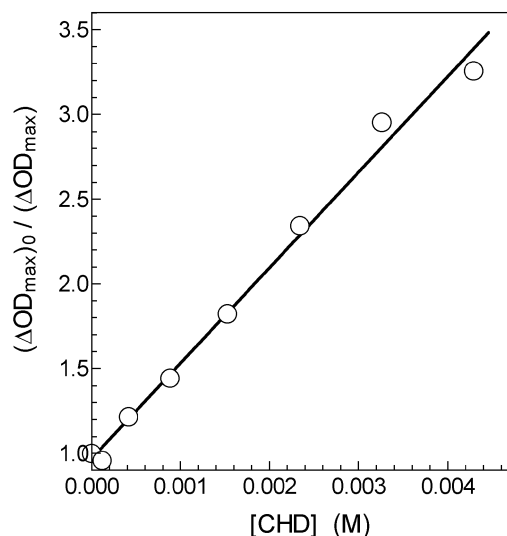


**Fig. 4.** Transient absorption spectrum from 248 nm laser flash photolysis of a deoxygenated  $2 \times 10^{-4}$  M solution of the phenolic ketone **6a** in dry acetonitrile solution at  $23.0 \pm 0.2^\circ\text{C}$ , corresponding to the peak of the decay profile ( $\Delta\text{OD}_{\text{max}}$ ). The insert shows a typical decay trace recorded at a monitoring wavelength of 385 nm.



In principle, hydrogen abstraction from phenols might be expected to proceed by at least three distinct mechanisms depending on the configuration and electronic structure of the lowest triplet state of the ketone, and the redox potentials of the ketone and the phenol in the particular solvent of interest. Two of these are analogous to those proposed for the photoreduction of benzophenone and acetophenone derivatives by substituted toluenes (13): (i) sequential electron and (or) proton-transfer (“ET–PT”) when electron transfer is sufficiently exergonic; (ii) when it is not, charge transfer assisted hydrogen abstraction (without prior hydrogen bonding), via an “*n*-type” exciplex for lowest  $n,\pi^*$  triplet ketones (“*nX*–HT”) or a “ $\pi$ -type” exciplex for lowest  $\pi,\pi^*$  triplets. In the latter cases, charge transfer from the phenol to the triplet ketone should increase the acidity of the phenolic

**Fig. 5.** Stern–Volmer quenching of the initial yield ( $\Delta\text{OD}_{\text{max}}$ ) of the transient from 337 nm laser flash photolysis of ketone **6a** (0.0015 M) in dry acetonitrile in the presence of various concentrations of 1,3-cyclohexadiene (CHD), monitored at 385 nm (see eq. [4]).



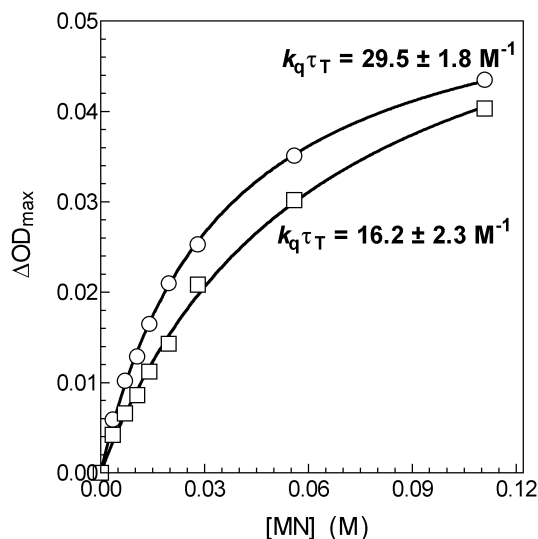
hydrogen and the basicity of the carbonyl oxygen, effectively enhancing the rate of hydrogen transfer above what might be expected on the basis of a “pure” hydrogen abstraction model. The third possibility (iii) involves the intermediacy of a hydrogen-bonded, “ $\pi$ -type” triplet exciplex that collapses to radicals by coupled electron- and proton-transfer (“HBX–EPT”). Reaction by this mechanism should be favored in ketones with particularly basic lowest triplet states, and hence should be fastest in ketones with lowest charge-transfer  $\pi,\pi^*$  triplet states. Reaction of  $n,\pi^*$  ketone triplets by this mechanism presumably requires the involvement of the higher lying  $\pi,\pi^*$  state, so will be fastest in those cases where the  $n,\pi^*-\pi,\pi^*$  triplet energy gap is small and the upper state is relatively basic. The three mechanistic possibilities are shown in Scheme 1.

The rate of reaction by any of these three mechanisms is expected to be sensitive to solvent polarity. It is well-known that reaction by the ET–PT (22, 23) and charge-transfer assisted (12, 13) mechanisms proceeds with enhanced rates as solvent polarity increases. In contrast, reaction by the HBX–EPT mechanism can be expected to be faster in solvents of low polarity, because hydrogen bonding is favored in nonpolar solvents. This leads to the conclusion that for the acetophenone and benzophenone chromophores, the triplet states of both isomers react via the HBX–EPT mechanism. This may also be true of the *meta,meta'*-phenolic indanone (**6a**), but the results for the *para,para'*-derivative (**3a**) are more consistent with a mechanism in which the phenolic hydrogen is activated toward abstraction by  $\pi$ -type charge transfer interactions between the aryl rings rather than by hydrogen-bonding.

The very slow rate of intramolecular hydrogen abstraction in **4a** compared to that in its *para,para'*-positional isomer **1a** has been proposed to result from a combination of conformational and orbital symmetry effects on the rate of electron/proton transfer within the hydrogen-bonded triplet

**Table 2.** Lifetimes (in ns) of carbonyl triplets in dry acetonitrile ( $[H_2O] \sim 1 \times 10^{-4}$  M), in acetonitrile containing 0.028 M  $H_2O$  and 0.028 M  $D_2O$ , and in dichloromethane at 23–25°C.<sup>a</sup>

Compound	R	MeCN	Wet MeCN <sup>b</sup>	$k_H/k_D^c$	$CH_2Cl_2$
<b>1</b>	H (a)	$12 \pm 2^d$	$14 \pm 2^d$	$1.3 \pm 0.2^d$	$2.2 \pm 0.3^e$
	Me (b)	$3500 \pm 200^d$	—	—	$3110 \pm 40$
<b>4</b>	H (a)	$11\,500 \pm 1800^{f,g}$	$7900 \pm 2300^{f,g}$	$1.2 \pm 0.2^f$	$1600 \pm 300^g$
	Me (b)	$8500 \pm 800^f$	—	—	$7040 \pm 180$
<b>2</b>	H (a)	$19 \pm 2^d$	$14 \pm 2^d$	$1.4 \pm 0.3^f$	$3.9 \pm 0.3^e$
	Me (b)	$5000 \pm 200^d$	—	—	$6400 \pm 110$
<b>5</b>	H (a)	$362 \pm 17^g$	$315 \pm 8^g$	$1.2 \pm 0.2^f$	$100 \pm 3$
	Me (b)	$9800 \pm 300$	—	—	$10\,500 \pm 400$
<b>3</b>	H (a)	$22 \pm 2^d$	$11 \pm 1^d$	$1.2 \pm 0.2^f$	$76 \pm 16^h$
	Me (b)	$281 \pm 4^d$	—	—	$445 \pm 8$
<b>6</b>	H (a)	$53 \pm 5^h$	$56 \pm 5^h$	$1.4 \pm 0.2^f$	$38 \pm 8^h$
	Me (b)	$970 \pm 20$	—	—	$1630 \pm 30$
<b>7</b>	—	$1370 \pm 20$	—	—	$1160 \pm 20$
<b>6c</b>	—	$3190 \pm 40$	—	—	$3660 \pm 60$

<sup>a</sup>Measured directly by 248 nm NLFP, using rigorously deoxygenated,  $0.8\text{--}1.2 \times 10^{-4}$  M solutions.<sup>b</sup>0.028 M  $H_2O$  in MeCN.<sup>c</sup>Ratio of lifetimes in acetonitrile containing 0.028 M  $D_2O$  and 0.028 M  $H_2O$ .<sup>d</sup>Data from ref. 11.<sup>e</sup>Determined using the 1-methylnaphthalene probe method (see Fig. 6).<sup>f</sup>Data from ref. 18.<sup>g</sup>At infinite dilution.<sup>h</sup>Estimated from the  $k_q\tau_T$  value for 1,3-cyclohexadiene quenching of biradical formation, obtained by 308 or 337 nm LFP of rigorously deoxygenate solutions, and using  $k_q$  values determined from quenching of model ketones (**12–17**) by 1,3-cyclohexadiene.**Fig. 6.** Plot of transient  $\Delta OD_{\max}$  vs. 1-methylnaphthalene concentration for **1a** ( $\square$ ) and **3a** ( $\circ$ ) in deoxygenated dichloromethane at  $25.0 \pm 0.2^\circ\text{C}$ . The solid lines represent the least-squares fits to eq. [5].

exciplex (**18**). Intramolecular hydrogen bonding in the lowest triplet state of **1a** can only take place in a conformer in which the two aryl rings are arranged in a sandwich-like structure; this obviously represents a “good” quenching geometry because the triplet lifetime of the molecule is so short. On the other hand, there are a number of conformers accessible to the *meta,meta'*-isomer (**4a**) which would allow hydrogen bonding between the phenolic hydrogen and the carbonyl oxygen, but in which there is little or no overlap between the  $\pi$ -systems of the two aryl rings. These are cal-

**Table 3.** Lifetimes (in ns) of the phenoxy-hemipinacol biradicals **20**, **21**, and **23–25** in dry acetonitrile ( $[H_2O] \sim 1 \times 10^{-4}$  M) and in dichloromethane at 23–25°C.<sup>a</sup>

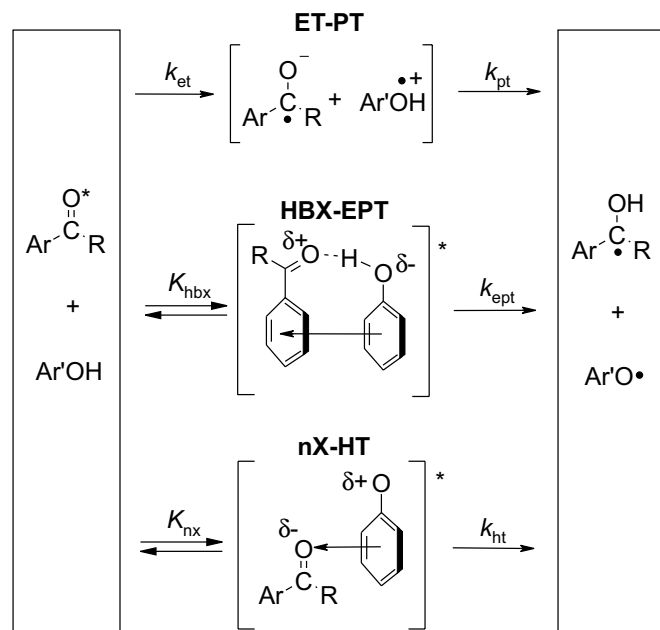
Biradical	MeCN	$CH_2Cl_2$
<b>23</b>	$170 \pm 20^b$	$120 \pm 15$
<b>24</b>	$285 \pm 35^b$	$360 \pm 40$
<b>20</b>	$830 \pm 90$	$450 \pm 50$
<b>25</b>	$90 \pm 10^b$	$120 \pm 20$
<b>21</b>	$630 \pm 70$	$590 \pm 60$

<sup>a</sup>Measured directly by 248 nm NLFP, using rigorously deoxygenated,  $0.8\text{--}1.2 \times 10^{-4}$  M solutions.<sup>b</sup>Data from ref. 11.

culated to be of considerably lower energy than the sandwich-like conformer analogous to that of **1a**, and hence should dominate the conformational equilibrium. This will lead to a much longer triplet lifetime if electron/proton transfer within these conformers is slow. Secondly, orbital overlap between the two phenyl rings in the (relatively high energy) sandwich-like exciplex conformer akin to **1a** is unfavorable, as a result of the nodal properties of the HOMO-1 and HOMO of the acceptor and donor, respectively. This can be expected to lead to a modest retardation of the rate of intramolecular electron transfer within the sandwich-like exciplex, relative to that in **1a** (24–30). At any rate, we consider the almost three-orders-of-magnitude difference between the triplet lifetimes of **4a** and **1a** to be a characteristic of intramolecular phenolic hydrogen abstraction by ketones tethered via *meta,meta'*- vs. *para,para'*-oxyethyl linkages, when the lowest triplet states are of the  $\pi\pi^*$  configuration and possess moderate charge transfer character.

The triplet decay rates of the *para,para'*-phenolic benzophenone derivative (**2a**) and its acetophenone counterpart

Scheme 1.



(1a) correlate with the relative rates of bimolecular hydrogen abstraction from *para*-cresol by the corresponding model compounds, *para*-methoxybenzophenone (**16**) and *para*-methoxyacetophenone (**17**), respectively. The slower rates of inter- and intramolecular reaction of the 4-alkoxybenzophenone derivatives compared to the 4-alkoxyacetophenones are suggested to be due to the fact that the former have lowest  $n,\pi^*$  triplet states, and are intrinsically less reactive than lowest  $\pi,\pi^*$  triplets of comparable reduction potential. As mentioned above, it is thought that they react as fast as they do because the lowest triplet state has some  $\pi,\pi^*$  character, the amount of which increases as the energy separation between the zero-order  $n,\pi^*$  and  $\pi,\pi^*$  states decreases. If this is true, then on the basis of the relative reactivities of **1a** and **4a**, one would expect the rate of intramolecular hydrogen abstraction in the *meta,meta'*-phenolic benzophenone **5a** to be significantly slower than in the *para,para'*-isomer **2a**, in agreement with the observed results.

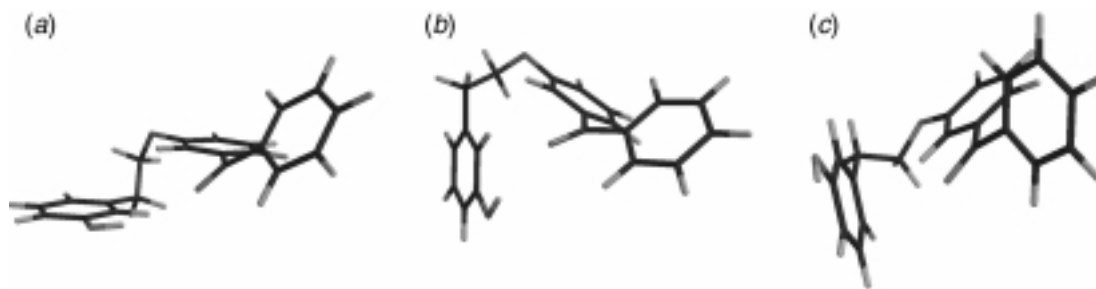
The rate deceleration caused by the *meta,meta'*-linkage in **5a** is at least an order of magnitude less pronounced than in the acetophenone series (**1a** and **4a**), however. The reason for this may be related to the fact that unlike the case with the acetophenone and indanone compounds, the bimolecular reactivity of the *meta,meta'*-pair (as defined by the rate of quenching of **12** by *meta*-cresol, see Table 1) is significantly higher than that of the *para,para'*-pair (i.e., **16** + *para*-cresol). This may be the result of the net electron-withdrawing character of the *meta*-alkoxy substituent, which places **12** (and **5a**) within the group of  $n,\pi^*$  benzophenone triplets in which the  $nX$ -HT mechanism is thought to be the predominant quenching pathway (11). In fact, molecular models indicate that the *meta,meta'*-linkage allows the facile formation of conformers in which the  $n$ -orbital of the carbonyl oxygen is directed into the  $\pi$ -system of the remote phenolic group. This is illustrated in Fig. 7, which shows

three of the possible quenching conformers available to **5a**: a displaced face-to-face conformer (a); a face-to-face conformer (b); and an  $n$ -type exciplex conformer (c). While the solvent effect on  $\tau_T$  (Table 2) suggests that the *main* quenching mechanism in **5a** is the same as in the *para,para'*-analogue **2a** (i.e., the HBX-EPT pathway), it is possible that quenching via the  $nX$ -HT mechanism competes to a small extent, resulting in somewhat higher reactivity than would be expected on the basis of the behavior of the *meta,meta'*-acetophenone derivative **4a**. Quenching via the  $nX$ -HT mechanism is geometrically impossible in the *para,para'*-analogue.

Even smaller differences in reactivity are observed for the *para,para'*- and *meta,meta'*-indanone derivatives (**3a** and **6a**), in spite of the fact that like **1a** and **4a**, both possess lowest  $\pi,\pi^*$  triplet states. The reason for this most likely originates in the coplanar arrangement of the carbonyl group and its associated aryl ring that is enforced by the benzannulated C-5 ring in these compounds. This results in a greater degree of charge-transfer in the  $\pi,\pi^*$  triplet state, which should have the effect of increasing its basicity. Thus, in the absence of geometric constraints, the rate of phenolic hydrogen abstraction should be higher than in the corresponding acetophenone derivatives if the quenching proceeds via the hydrogen-bonded exciplex mechanism. Indeed, the rate constants for bimolecular phenolic hydrogen abstraction by the model compounds **13** and **15** are significantly higher than those for the analogous acetophenone derivatives **14** and **17**, respectively, (see Table 1). In spite of this, intramolecular abstraction in the *para,para'*-derivative **3a** is significantly slower than in the acetophenone **1a**, a result which has been attributed to the less than optimal geometry for intramolecular hydrogen bonding that is enforced at the carbonyl group by the benzannulated C-5 ring. The fact that the triplet lifetime of **3a** is increased in dichloromethane relative to acetonitrile suggests that this explanation is correct, and hydrogen bonding is indeed not involved in the dominant quenching mechanism for this compound. This problem should be much less severe in **6a**, because the *meta,meta'*-linkage allows hydrogen bonding between the carbonyl and the remote phenolic group to occur with much greater facility than in the *para,para'*-derivatives.

Also relevant to this discussion are the unusually short triplet lifetimes of the anisyl derivatives of these two ketones, which indicates that they possess a route for nonproductive intramolecular triplet deactivation that is not present to the same extent in the corresponding acetophenone and benzophenone derivatives. For example, the triplet lifetimes of **3b** ( $\tau_T = 280$  ns) and **6b** ( $\tau_T = 970$  ns) in deoxygenated acetonitrile are more than an order of magnitude shorter than those of **15** and **13** under the same conditions ( $\tau_T > 10$   $\mu$ s), while those of the phenyl-derivatives **7** ( $\tau_T = 1.4$   $\mu$ s) and **6c** ( $\tau_T = 3.2$   $\mu$ s) are intermediate between these extremes. These effects appear to be strictly confined to the intramolecular systems, since the bimolecular rate constants for 1,4-dimethoxybenzene quenching of the triplet states of **15** ( $k_q = (4.8 \pm 0.8) \times 10^7$   $M^{-1} s^{-1}$ ) and **13** ( $k_q = (1.8 \pm 0.4) \times 10^7$   $M^{-1} s^{-1}$ ) in acetonitrile are nearly identical to the corresponding values for the acetophenone homologues **17** ( $k_q = (4.4 \pm 0.4) \times 10^7$   $M^{-1} s^{-1}$ ) and

**Fig. 7.** Potential quenching geometries for **5a**: (a) lowest energy H-bonded conformer; (b) sandwich-like H-bonded conformer; (c) *n*-type exciplex conformer.



**14** ( $k_q = (2.2 \pm 0.2) \times 10^7 \text{ M}^{-1} \text{ s}^{-1}$ ), respectively, under the same conditions.<sup>2</sup> A charge transfer quenching mechanism, presumably via the  $\pi$ -type triplet exciplex pathway first suggested by Singer and co-workers (31), is suggested by the fact that the triplet lifetimes of the four compounds are longer in the less polar solvent dichloromethane. Certainly, (endothermic) triplet energy transfer can most likely be ruled out as a possibility. We suspect that the reason for the enhanced intramolecular charge transfer quenching in the indanone series compared to the acetophenones may be related to exciplex structure; the results suggest that the optimum exciplex geometry for charge transfer between the aroyl and the donor aryl rings is somewhat different in the indanones than in the acetophenones, with that in the former being more compatible with the orientational constraints placed on the molecules by the oxyethyl tether in the intramolecular systems. In any event, the solvent effects on the triplet lifetimes of **3a** and **6a** suggest that this mechanism dominates over the hydrogen-bonded exciplex mechanism in **3a** (in which geometric factors prevent in-plane bonding between the carbonyl oxygen and the phenolic hydrogen); but only competes with it in **6a**, where these constraints are relaxed.

## Summary and conclusions

The intriguing geometry dependence on the rate constants for remote phenolic hydrogen abstraction in the  $\pi, \pi^*$  triplet states of the *para,para'*- and *meta,meta'*-oxyethyl linked phenolic ketones **1a** and **4a** has been investigated in the corresponding benzophenone ( $n, \pi^*$  lowest triplet) and indanone (CT- $\pi, \pi^*$  lowest triplet) homologues. Solvent effects on the triplet lifetimes suggest that all ketones in the series but one react mainly via a hydrogen-bonded triplet exciplex, which collapses to the corresponding biradical by coupled electron and (or) proton transfer.

The new compounds exhibit similar structural dependences on intramolecular reactivity as observed for the acetophenone derivatives **1a** and **4a**, but the differences between *meta,meta'*- and *para,para'*-positional isomers are an order of magnitude smaller for the benzophenone derivatives (**2a** and **5a**), and two orders of magnitude smaller for the indanones (**3a** and **6a**). In the benzophenone case, the higher than expected reactivity of the *meta,meta'*-isomer may be due to competing reaction via the *n*-type exciplex ( $nX$ -HT) mechanism analogous to that involved in the quenching of benzophenone  $n, \pi^*$  triplets by substituted toluenes. The even

higher relative reactivity of the *meta,meta'*-indanone derivative is proposed to be due to more facile charge transfer between the two aryl rings in the hydrogen-bonded exciplex associated with this compound. In the *para,para'*-isomer, on the other hand, a relatively poor geometry for intramolecular hydrogen bonding is enforced by the benzannulated C-5 ring, which prevents the remote O—H bond from adopting a coplanar arrangement with the carbonyl group. As a result, hydrogen abstraction is initiated by a simple charge transfer interaction between the electron-rich phenolic ring and the indanone moiety, which increases the acidity of the phenolic hydrogen and activates its transfer. Supporting evidence for this conclusion is derived from the behavior of analogues bearing remote anisyl groups, which exhibit significantly shorter triplet lifetimes than do the corresponding anisyl-substituted acetophenone derivatives.

Future work in this area will further address the factors responsible for the substantial structural dependence on the rates of intramolecular phenolic hydrogen abstraction in acetophenone derivatives, and explore the mechanisms of the bimolecular process in aromatic ketones of various structure.

## Experimental

<sup>1</sup>H and <sup>13</sup>C NMR spectra were recorded on Bruker AC200 (200 MHz) or AC300 (300 MHz) spectrometers in deuterated solvents, and are reported in ppm downfield from tetramethylsilane. Ultraviolet absorption spectra were recorded on Cary 50 or Cary 300 UV-vis spectrophotometers. Mass spectra and exact masses were recorded on a VG Analytical ZABE mass spectrometer employing a mass of 12.000000 for carbon. Infrared spectra were recorded on a Biorad FTS-40 FT IR spectrometer. Melting points were determined on a polarizing microscope fitted with a Mettler hot stage and Mettler FP80 processor, and are not corrected. Gas chromatographic analyses employed a Hewlett-Packard 5890 Series 2 gas chromatograph equipped with a flame ionization detector, a Hewlett-Packard 3396A recording integrator, and a 15 m × 0.53 mm DB-17A or 5 m × 0.53 mm HP-1 column (Chromatographic Specialties, Inc.). Radial chromatography was carried out using a Chromatotron<sup>®</sup> (Harrison Research) with 4 mm silica gel 60 (EM Science) thick-layer plates. Elemental analyses were carried out by Guelph Chemical Laboratories, Inc.

Acetone (Caledon Reagent) was dried over anhydrous potassium carbonate and freshly distilled before use, hexanes

<sup>2</sup>E.C. Lathioor, and W.J. Leigh. Unpublished results.

(Caledon Reagent) were distilled, acetonitrile (Caledon reagent) was distilled from calcium hydride and passed repeatedly through activated Brockmann alumina (Aldrich), and pyridine (Fisher Reagent) was distilled from barium oxide. All other solvents were reagent grade and were used as received from the suppliers (Caledon or Fisher).

*meta*-Cresol (Caledon) and 3-hydroxybenzophenone (Aldrich) were used as received, while 1,3-cyclohexadiene (Aldrich) was bulb-to-bulb distilled and stored at  $-20^{\circ}\text{C}$  under argon. 6-Hydroxy-1-indanone was prepared by demethylating 6-methoxy-1-indanone (Aldrich) with  $\text{AlCl}_3$  as described by Miyake et al. (32), followed by recrystallization from water. 3-Methoxybenzophenone was prepared by Friedel–Crafts acylation of benzene with *meta*-anisoyl chloride, and purified by silica gel chromatography. 1-Bromo-2-(3-methoxyphenyl)ethane and 1-tosyloxy-2-(3-tosyloxyphenyl)ethane were prepared as previously described (18).

### 3-[2-(3-Hydroxyphenyl)ethoxy]benzophenone (5a)

To a 100 mL round-bottom flask attached to a reflux condenser and equipped with a magnetic stir bar was added anhydrous acetone (50 mL), 3-hydroxybenzophenone (1 g, 0.005 mol), 1-tosyloxy-2-(3-tosyloxyphenyl)ethane (4.50 g, 0.011 mol), and anhydrous potassium carbonate (0.87 g, 0.006 mol). The mixture was refluxed for 72 h, after which it was stripped of solvent on the rotary evaporator, acidified with dilute HCl until gas evolution ceased, and then taken up in ethyl acetate (50 mL). The orange-colored organic phase was then washed with water ( $2 \times 50$  mL) and saturated brine (50 mL), dried with anhydrous magnesium sulfate, filtered, and concentrated under reduced pressure. The crude tosylate ester was hydrolyzed by dissolving in methanol (100 mL) containing potassium carbonate (10 g, 0.07 mol) and refluxing for 80 h. Work-up as before yielded 2.54 g of a light brown oil consisting of a mixture of the desired product with minor amounts of 3-hydroxystyrene. Purification by radial chromatography (30% ethyl acetate in hexanes as eluant), followed by column chromatography (3% ether in dichloromethane with 10 drops acetic acid/100 mL as eluant) yielded a colorless oil (1.2 g, 0.0040 mol, 80%) which was identified as **5a** on the basis of the following data. MS (*m/e*) (I): 318 (10), 199 (3), 121 (100), 105 (23), 91 (16), 77 (45), 65 (8), 51(8). HRMS calcd. for  $\text{C}_{21}\text{H}_{18}\text{O}_3$ : 318.12564; found: 318.125592. UV  $\lambda_{\text{max}}$  (MeCN) (nm): 220 ( $\epsilon$  27 600  $\text{M}^{-1} \text{cm}^{-1}$ ), sh. 253, 307. IR (KBr,  $\text{cm}^{-1}$ ): 3413 (br m), 3064 (w), 2934 (w), 2875 (w), 1716 (s), 1661 (s), 1594 (s), 1489 (w), 1451 (m), 1363 (m), 1287 (s), 1224 (s), 1161 (w), 1039 (w), 876 (w), 787 (w), 728 (m), 708 (m), 535 (w).  $^1\text{H}$  NMR ( $\text{CDCl}_3$ )  $\delta$ : 3.00 (t,  $J = 7$  Hz, 2H), 4.14 (t,  $J = 7$  Hz, 2H), 6.2 (s, 1H), 6.7–6.85 (m, 3H), 7.1–7.2 (m, 2H), 7.3–7.6 (m, 6H), 7.79 (d,  $J = 8$  Hz, 2H).  $^{13}\text{C}$  NMR ( $\text{CDCl}_3$ )  $\delta$ : 35.4, 68.6, 113.6, 115.0, 116.0, 119.6, 121.1, 123.0, 128.3, 129.2, 129.6, 130.1, 132.6, 137.3, 138.6, 139.7, 155.9, 158.7, 197.2. Anal. calcd. for  $\text{C}_{21}\text{H}_{18}\text{O}_3$ : C 79.22, H 5.70; found: C 79.52, H 5.85.

### 6-[2-(3-Hydroxyphenyl)ethoxy]-1-indanone (6a)

To a 100 mL round-bottom flask attached to a reflux condenser and equipped with a magnetic stir bar was added anhydrous acetone (50 mL), 6-hydroxy-1-indanone (0.68 g,

0.00459 mol), anhydrous potassium carbonate (1.42 g, 0.0103 mol), and 1-tosyloxy-2-(3-tosyloxyphenyl)ethane (2.24 g, 0.00510 mol). The mixture was refluxed with stirring for 10 h, additional quantities of potassium carbonate (0.71 g, 0.005 mol) and the ditosylate (1.02 g, 0.0023 mol) were added, and the reflux continued for a further 60 h. The reaction mixture was stripped of solvent on the rotary evaporator and then acidified with dilute HCl until gas evolution ceased. The aqueous mixture was extracted with ethyl acetate (50 mL), which caused the formation of an emulsion that was clarified with the addition of brine (25 mL). The orange-colored organic phase was washed with water ( $2 \times 80$  mL) and saturated brine (100 mL), dried with anhydrous magnesium sulfate, filtered, and concentrated under reduced pressure. The mixture was then taken up in methanol (25 mL), potassium carbonate (5.0 g, 0.04 mol) was added, and the resulting solution was refluxed for 48 h. Work-up as above yielded a deep brown oil (1.76 g). Column chromatography on silica gel with chloroform as eluant yielded compound **6a** (0.34 g, 0.0013 mol, 30%) as light yellow crystals, which were recrystallized from chloroform–cyclohexane with 1% methanol (mp  $135.5$  to  $136.0^{\circ}\text{C}$ ) and identified on the basis of the following data. MS (*m/e*) (I): 268 (25), 121 (100), 103 (31), 91 (39), 77 (44), 65 (12). HRMS calcd. for  $\text{C}_{17}\text{H}_{16}\text{O}_3$ : 268.1072; found: 268.1099. UV  $\lambda_{\text{max}}$  (MeCN) (nm): 219 ( $\epsilon$  32 650  $\text{M}^{-1} \text{cm}^{-1}$ ) 244 (sh), 275, 280, 317. IR (KBr,  $\text{cm}^{-1}$ ): 3417 (br m), 3278 (w), 3051 (w), 3009 (w), 2938 (w), 1716 (s), 1690 (m), 1623 (w), 1590 (w), 1493 (w), 1364 (m), 1287 (m), 1224 (m), 1161 (w), 1090 (w), 1040 (w), 951 (w), 838 (w), 703 (w), 527 (w).  $^1\text{H}$  NMR ( $\text{CD}_3\text{CN}$ )  $\delta$ : 2.60–2.64 (m, 3H), 2.97–3.06 (m, 4H), 4.22 (t,  $J = 7$  Hz, 2H), 6.65–6.70 (m, 1H), 6.8 (m, 2H), 7.08–7.2 (m, 2H), 7.41 (d,  $J = 8$  Hz, 1H), 7.74 (d,  $J = 3$  Hz, 1H).  $^{13}\text{C}$  NMR ( $\text{CD}_3\text{CN}$ )  $\delta$ : 25.4, 35.9, 37.3, 69.6, 95.0 106.5, 114.0, 116.6, 121.0, 124.2, 128.4, 130.1, 139.0, 140.9, 148.7, 158.0, 159.3. Anal. calcd. for  $\text{C}_{17}\text{H}_{16}\text{O}_3$ : C 76.10, H 6.01; found: C 75.50, H 6.07.

### 3-[2-(3-Methoxyphenyl)ethoxy]benzophenone (5b)

A mixture of 3-hydroxybenzophenone (2.50 g, 0.0126 mol), 1-bromo-2-(3-methoxyphenyl)ethane (4.79 g, 0.0223 mol), and anhydrous potassium carbonate (1.74 g, 0.013 mol) were combined in acetone (20 mL), and stirred under reflux for 16 h. A second portion of potassium carbonate (0.50 g, 0.0036 mol) was added, and the mixture was refluxed for a further 4 days. The reaction was still not complete, so additional potassium carbonate (0.025 g, 0.0018 mol) and bromide (2.02 g, 0.009 mol) were added and reflux was continued for another 5 days. The  $^1\text{H}$  NMR spectrum of a portion of the reaction mixture (after work-up as described below) indicated only 80% consumption of the 3-hydroxybenzophenone starting material, so an additional portion of bromide (1.09 g, 0.005 mol) was added and the mixture was refluxed for a further 3 days. The reaction mixture was cooled, and then taken up in a mixture of 1:1 ether:ethyl acetate (50 mL) and water (50 mL). The layers were separated, the aqueous portion was acidified with 3 M HCl, and extracted with ether (50 mL) and ethyl acetate ( $2 \times 25$  mL). The combined organic layers were washed with water (200 mL), 5% aq sodium bicarbonate (100 mL) and brine (100 mL), dried over anhydrous magnesium sulfate, and fil-

tered. Removal of the organic solvents on the rotary evaporator yielded an orange-brown oil, which was purified by silica gel column chromatography using 1:1 hexane:dichloromethane as eluant to yield a yellow oil (2.73 g, 0.008 mol, 65%). The compound was identified as **5b** on the basis of the following data. MS (*m/e*) (I): 332(10), 135(100), 120(7), 105(56), 91(28), 77(68), 65(12), 51(16). HRMS calcd. for C<sub>22</sub>H<sub>20</sub>O<sub>3</sub>: 332.1413; found: 332.1413. UV λ<sub>max</sub> (MeCN) (nm): 220 nm (ε 28 300 M<sup>-1</sup> cm<sup>-1</sup>), sh. 252, 305. IR (KBr, cm<sup>-1</sup>): 3060 (w), 2939 (w), 2835 (w), 1658 (m), 1596 (m), 1488 (m), 1438 (m), 1281 (s), 1164 (m), 1043 (s), 971 (w), 872 (w), 781 (s), 724 (s). <sup>1</sup>H NMR (CDCl<sub>3</sub>) δ: 3.07 (t, 2H, *J* = 7 Hz), 3.77 (s, 3H), 4.20 (t, 2H, *J* = 7 Hz), 6.75–6.86 (m, 3H), 7.08–7.12 (m, 1H), 7.20 (d, 1H, *J* = 8 Hz), 7.31–7.35 (m, 3H), 7.42–7.47 (m, 2H), 7.53–7.58 (m, 1H), 7.76–7.79 (m, 2H). <sup>13</sup>C NMR (CDCl<sub>3</sub>) δ: 35.6, 55.0, 68.6, 111.7, 114.7, 115.0, 119.2, 121.2, 122.7, 128.1, 129.1, 129.4, 129.9, 132.3, 137.7, 138.7, 139.5, 158.6, 159.6, 196.3. Anal. calcd. for C<sub>20</sub>H<sub>22</sub>O<sub>3</sub>: C 79.50, H 6.06; found: C 79.90, H 5.93.

#### 6-[2-(3-Methoxyphenyl)ethoxy]-1-indanone (**6b**)

To a 25 mL round-bottom flask fitted with a condenser, nitrogen inlet, and magnetic stirrer was added anhydrous potassium carbonate (0.47 g, 0.0034 mol), acetone (10 mL), 6-hydroxy-1-indanone (0.46 g, 0.0034 mol), and 1-bromo-2-(3-methoxyphenyl)ethane (1.51 g, 0.007 mol). The mixture was refluxed under a nitrogen atmosphere for 10 days, with periodic monitoring by TLC. Additional quantities of acetone (10 mL) and potassium carbonate (0.50 g) were added, and the mixture was then refluxed for a further 5 days. The mixture was filtered and the solvent was removed on the rotary evaporator to yield a red oil, which was taken up in ether (50 mL) and 2% aq HCl (50 mL). The layers were separated, and the aqueous fraction was extracted with ether (2 × 50 mL). The organic fractions were combined, washed with water (100 mL) and brine (100 mL), dried with anhydrous magnesium sulfate, and filtered. Removal of the ether under reduced pressure yielded an orange oil (1.4 g), which was purified by column chromatography using 10% ethyl acetate in hexanes as eluant, followed immediately by column chromatography using chloroform as an eluant. The product was obtained as a yellow oil (0.47 g, 0.0016 mol, 53%), which was identified as **6b** on the basis of the following data. <sup>1</sup>H NMR (CDCl<sub>3</sub>) δ: 2.61 (m, 2H), 3.00 (m, 4H), 3.71 (s, 3H), 4.12 (t, *J* = 7 Hz, 2H), 6.65–6.72 (m, 1H), 6.8 (m, 2H), 7.08–7.2 (m, 3H), 7.22 (d, *J* = 8 Hz, 1H), 7.74 (d, *J* = 3 Hz, 1H). <sup>13</sup>C NMR (CDCl<sub>3</sub>) δ: 25.1, 35.6, 37.0, 68.9, 105.9, 111.9, 114.8, 121.3, 124.3, 127.4, 128.3, 129.5, 138.2, 139.6, 148.0, 158.6, 159.8, 206.9. UV λ<sub>max</sub> (MeCN) (nm): 218 (ε 29 250 M<sup>-1</sup> cm<sup>-1</sup>), sh. 243, 272, 279, 315. IR (KBr, cm<sup>-1</sup>): 3005 (w), 2925 (w), 2837 (w), 1711 (s), 1613 (w), 1492 (m), 1446 (w), 1296 (m), 1275 (m), 1222 (m), 1168 (w), 1155 (w), 1040 (m), 837 (w), 785 (w), 697 (w), 558 (w), 530 (w). MS (*m/e*) (I): 282 (18), 135 (100), 120 (8), 105 (25), 91 (30), 67 (27), 65 (22), 51 (12), 43 (33). HRMS calcd. for C<sub>18</sub>H<sub>18</sub>O<sub>3</sub>: 282.1256; found: 282.1256. Anal. calcd. for C<sub>18</sub>H<sub>18</sub>O<sub>3</sub>: C 76.57, H 6.43; found: C 76.74, H 6.61.

#### 6-[2-(Phenyl)ethoxy]-1-indanone (**6c**)

To an oven-dried 100-mL round-bottom flask equipped with magnetic stirrer, reflux condenser, and nitrogen inlet was added freshly distilled acetone (50 mL), 1-tosyloxy-2-phenylethane (0.50 g, 0.0018 mol), anhydrous potassium carbonate (0.28 g, 0.002 mol), and 6-hydroxy-1-indanone (0.24 g, 0.0016 mol). The mixture was then refluxed under nitrogen for 48 h. The dark brown mixture was stripped of solvent to leave a grey-brown residue, which was acidified by the addition of 0.4 M H<sub>2</sub>SO<sub>4</sub> (20 mL) and concd HCl (1 mL), and then extracted with a mixture of ether (50 mL) and benzene (5 mL). The resulting bright yellow organic phase was washed with 10% aq NaOH (30 mL), water (30 mL), and brine (30 mL), and then dried with anhydrous magnesium sulfate. The solvent was removed under reduced pressure to yield an orange semisolid (0.44 g), which was recrystallized from methanol to yield yellow needles (mp 69.0–71°C; 0.26 g, 0.001 mol, 64%). The compound was identified as **6c** on the basis of the following data. MS (*m/e*) (I): 252 (10), 105 (100), 91 (13), 79 (20), 77 (23), 65 (7), 51 (10). HRMS calcd. for C<sub>17</sub>H<sub>16</sub>O<sub>2</sub>: 252.115028; found: 252.115080. UV λ<sub>max</sub> (MeCN): 205 (ε 24 555 M<sup>-1</sup> cm<sup>-1</sup>), 213 (ε 24 691 M<sup>-1</sup> cm<sup>-1</sup>), 244 (ε 8200 M<sup>-1</sup> cm<sup>-1</sup>), 316 (ε 3600 M<sup>-1</sup> cm<sup>-1</sup>). IR (KBr, cm<sup>-1</sup>): 3061 (vw), 2948 (w), 2918 (w), 1705 (vs), 1620 (w), 1491, 1447, 1297, 1254, 1226, 1196 (w), 1170 (w), 1018, 918 (vw), 835, 720, 696. <sup>1</sup>H NMR (CDCl<sub>3</sub>) δ: 2.65 (t, 2H, *J* = 6 Hz), 2.98–3.09 (m, 5H), 4.15 (t, 2H, *J* = 7 Hz), 7.09–7.32 (m, 8H). <sup>13</sup>C NMR (CDCl<sub>3</sub>) δ: 25.3, 35.7, 37.1, 69.2, 106.1, 124.5, 126.7, 127.5, 128.7, 129.1, 138.2, 138.4, 148.1, 158.7, 207.0. Anal. calcd. for C<sub>17</sub>H<sub>16</sub>O<sub>2</sub>: C 80.93, H 6.39; found: C 80.64, H 6.59.

#### 5-[2-(Phenyl)ethoxy]-1-indanone (**7**)

This compound was prepared in analogous fashion to **6c**, from 1-tosyloxy-2-phenylethane (1.16 g, 0.0042 mol), 5-hydroxy-1-indanone (0.61 g, 0.0041 mol), and anhydrous potassium carbonate (0.70 g, 0.005 mol) in dry acetone (50 mL). After refluxing under nitrogen for 5 days, the reaction mixture was worked up as above to yield an orange solid (1.09 g), which was recrystallized from methanol to yield a pale yellow powder (mp 79 to 79.5°C; 0.48 g, 0.0019 mol, 46%). The compound was identified as **7** on the basis of the following data. <sup>1</sup>H NMR (CDCl<sub>3</sub>) δ: 2.59 (t, 2H, *J* = 6 Hz), 2.99 (t, 2H, *J* = 6 Hz), 3.06 (t, 2H, *J* = 7 Hz), 4.18 (t, 2H, *J* = 7 Hz), 6.83 (d, 2H, *J* = 6 Hz), 7.18–7.27 (m, 5H), 7.61 (d, 1H, *J* = 9 Hz). <sup>13</sup>C NMR (CDCl<sub>3</sub>) δ: 26.0, 35.7, 36.5, 69.2, 110.6, 115.7, 125.5, 126.8, 128.7, 129.1, 130.6, 137.9, 158.1, 164.6, 205.2. UV λ<sub>max</sub> (MeCN): 200 (ε 24 500 M<sup>-1</sup> cm<sup>-1</sup>), 220 (ε 17 000 M<sup>-1</sup> cm<sup>-1</sup>), 264 (ε 17 800 M<sup>-1</sup> cm<sup>-1</sup>), 287 (ε 10 000 M<sup>-1</sup> cm<sup>-1</sup>), 295 (ε 10 000 M<sup>-1</sup> cm<sup>-1</sup>). IR (KBr, cm<sup>-1</sup>): 3060 (vw), 3039 (vw), 2938 (w), 2908(w), 1702 (vs), 1593 (s), 1489, 1460, 1440, 1303, 1255 (vs), 1140, 1089, 1013, 855, 835, 806, 760, 708, 643 (w), 588, 535 (vw). MS (*m/e*) (I): 252 (17), 105 (100), 91 (15), 79 (25), 77 (33), 65 (11), 51 (13). HRMS calcd. for C<sub>17</sub>H<sub>16</sub>O<sub>2</sub>: 252.115028; found: 252.110220. Anal. calcd. for C<sub>17</sub>H<sub>16</sub>O<sub>2</sub>: C 80.93, H 6.39; found: C 81.09, H 6.52.

Nanosecond laser flash photolysis experiments employed the pulses from a Lumonics TE-861M excimer laser filled

with Xe-HCl-H<sub>2</sub>He (308 nm, 15 ns, ca. 40 mJ) or N<sub>2</sub>-He (337 nm, 6 ns, ca. 4 mJ), a Lumonics 510 excimer laser filled with Kr-F<sub>2</sub>-He (248 nm, 20 ns, ca. 60 mJ), or a Lambda Physik Compex 120 filled with Kr-F<sub>2</sub>-Ne (248 nm, 25 ns, 100–140 mJ), and a computer-controlled detection system which has been described elsewhere (17, 19). All samples were contained in 3 × 7 mm or 7 × 7 mm Suprasil quartz cells which were sealed with rubber septa. Substrate concentrations were adjusted to yield an absorbance between 0.2 and 0.9 at the excitation wavelength. Each solution was deoxygenated with dry nitrogen or argon until constant lifetimes were achieved. Quenchers were added as aliquots of standard solutions.

Phosphorescence emission spectra were determined with either a PerkinElmer LS-5 or Photon Technologies LS-100 spectrofluorimeter. Sample concentrations were ~1 mg mL<sup>-1</sup> and were contained in 2-mm i.d. Suprasil quartz tubes that were sealed with rubber septa and deoxygenated with dry nitrogen.

Steady-state irradiations were performed in a Rayonet Reactor (New England Ultraviolet Co.) using RPR-300 lamps and a merry-go-round apparatus. Samples were contained in 3-mm i.d. quartz tubes sealed with rubber septa, and were deoxygenated with nitrogen. Progress of the photolyses was monitored periodically by GC using the disappearance of **1a** as an actinometer. Hexadecane was employed as an internal standard.

Semiempirical (AM1) calculations were carried out using Spartan<sup>TM</sup> 5.0.3 (Wavefunction, Inc.) on a dual-processor Silicon Graphics Octane workstation. The (ground state) hydrogen-bonded conformers of Figs. 7a, 7b ( $\Delta H_f = -39.61$  and  $-40.19$  kcal mol<sup>-1</sup>, respectively) were minimized with the OH—OC distance constrained at 2.60 Å, while the *n*-type exciplex conformer of Fig. 7c ( $\Delta H_f = -36.50$  kcal mol<sup>-1</sup>) was minimized with a constrained distance of 3.60 Å between the carbonyl oxygen and the *ortho*- (with respect to the linker group) carbons of the remote phenolic ring.

## Acknowledgements

We thank the Natural Sciences and Engineering Research Council of Canada (NSERC) for financial support of this work.

## References

1. N.J. Turro and R. Engel. *J. Am. Chem. Soc.* **91**, 7113 (1969).
2. N.J. Turro and T.J. Lee. *Mol. Photochem.* **2**, 185 (1970).
3. P.K. Das, M.V. Encinas, and J.C. Scaiano. *J. Am. Chem. Soc.* **103**, 4154 (1981).
4. R. Das, R. Bhatnagar, and B. Venkataraman. *Proc. Indian Acad. Sci. Chem. Sci.* **106**, 1681 (1994).
5. L. Biczok, T. Berces, and H. Linschitz. *J. Am. Chem. Soc.* **119**, 11 071 (1997).
6. S.V. Jovanovic, D.G. Morris, C.N. Pliva, and J.C. Scaiano. *J. Photochem. Photobiol. A*, **107**, 153 (1997).
7. P.J. Wagner and B.-S. Park. *Org. Photochem.* **11**, 227 (1991).
8. S. Canonica, U. Jans, K. Stemmler, and J. Hoigne. *Environ. Sci. Technol.* **29**, 1822 (1995).
9. S. Canonica, B. Hellrung, and J. Wirz. *J. Phys. Chem. A*, **104**, 1226 (2000).
10. P.H. Given, M.E. Poever, and J. Schoen. *J. Chem. Soc.* 2674 (1958).
11. W.J. Leigh, E.C. Lathioor, and M.J. St. Pierre. *J. Am. Chem. Soc.* **118**, 12 339 (1996).
12. P.J. Wagner and R.A. Leavitt. *J. Am. Chem. Soc.* **95**, 3669 (1973).
13. P.J. Wagner, R.J. Truman, A.E. Puchalski, and R. Wake. *J. Am. Chem. Soc.* **108**, 7727 (1986).
14. P. Jacques, X. Allonas, M. von Raumer, P. Suppan, and E. Haselbach. *J. Photochem. Photobiol. A*, **111**, 41 (1997).
15. P. Jacques. *J. Photochem. Photobiol. A*, **56**, 159 (1991).
16. J.C. Scaiano, W.G. McGimpsey, W.J. Leigh, and S. Jakobs. *J. Org. Chem.* **52**, 4540 (1987).
17. W.J. Leigh, M.S. Workentin, and D. Andrew. *J. Photochem. Photobiol. A*, **57**, 97 (1991).
18. E.C. Lathioor, W.J. Leigh, and M.J. St. Pierre. *J. Am. Chem. Soc.* **121**, 11 984 (1999).
19. C.J. Bradaric and W.J. Leigh. *Can. J. Chem.* **75**, 1393 (1997).
20. G. Beck, G. Dobrowolski, J. Kiwi, and W. Schnabel. *Macromolecules*, **8**, 9 (1975).
21. J.P. Bays, M.V. Encinas, and J.C. Scaiano. *Macromolecules*, **13**, 815 (1980).
22. S. Inbar, H. Linschitz, and S.G. Cohen. *J. Am. Chem. Soc.* **103**, 1048 (1981).
23. S. Inbar, H. Linschitz, and S.G. Cohen. *J. Am. Chem. Soc.* **104**, 1679 (1982).
24. R.L.J. Zsom, L.G. Schroff, C.J. Bakker, J.W. Verhoeven, Th. J. De Boer, J.D. Wright, and H. Kuroda. *Tetrahedron*, **34**, 3225 (1978).
25. H.A. Staab and W. Rebafka. *Chem. Ber.* **110**, 3333 (1977).
26. H.A. Staab, C.P. Herz, C. Krieger, and M. Rentea. *Chem. Ber.* **110**, 3351 (1977).
27. H.A. Staab, C.P. Herz, C. Krieger, and M. Rentea. *Chem. Ber.* **116**, 3813 (1983).
28. Y. Sakata, H. Tsue, Y. Goto, S. Misumi, T. Asahi, S. Nishikawa, T. Okada, and N. Mataga. *Chem. Lett.* 1307 (1991).
29. N. Helsen, L. Viaene, M. Van der Auweraer, and F.C. De Schryver. *J. Phys. Chem.* **98**, 1532 (1994).
30. T. Fiebig, W. Kuhnle, and H. Staerk. *Chem. Phys. Lett.* **282**, 7 (1998).
31. M.W. Wolf, R.E. Brown, and L.A. Singer. *J. Am. Chem. Soc.* **99**, 526 (1977).
32. A. Miyake, K. Itoh, N. Tada, M. Tanabe, M. Hirata, and Y. Oka. *Chem. Pharm. Bull.* **31**, 2329 (1983).